

# Spatial distribution of rare-earth ions and GaS<sub>4</sub> tetrahedra in chalcogenide glasses studied via laser spectroscopy and *ab initio* molecular dynamics simulation

T. H. Lee,<sup>1</sup> S. I. Simdyankin,<sup>1,2</sup> J. Hegedus,<sup>1</sup> J. Heo,<sup>3</sup> and S. R. Elliott<sup>1</sup><sup>1</sup>Department of Chemistry, University of Cambridge, Lensfield Road, Cambridge CB2 1EW, United Kingdom<sup>2</sup>WPI Advanced Institute for Materials Research, Tohoku University, 2-1-1 Katahira, Aoba-ku, Sendai 980-8577, Japan<sup>3</sup>Center for Information Materials and Department of Materials Science and Engineering, Pohang University of Science and Technology, Pohang, Kyungbuk 790-784, Korea

(Received 19 January 2010; published 16 March 2010)

The spatial distribution of Nd<sup>3+</sup> ions and GaS<sub>4</sub> tetrahedral units in Nd-doped Ge-As-Ga-S glasses has been studied by laser spectroscopy and *ab initio* molecular dynamics (MD) simulations. A sharp increase in Nd<sup>3+</sup> fluorescence intensities and lifetimes was observed with increasing Ga content, and attributed to the formation of tightly bound Nd<sup>3+</sup> clusters in Ga-free glasses and the subsequent dissolution of such clusters upon Ga doping. A large modification in Nd<sup>3+</sup> sites was also identified from low-temperature site-selective excitation spectra, suggesting preferential spatial correlations between Nd<sup>3+</sup> and GaS<sub>4</sub> tetrahedra even at low Ga-doping levels. MD simulations of these materials in the liquid state showed a tendency for Ga cluster formation as well as spatial correlations between Nd and Ga atoms consistent with the experimental results. On the basis of this result, a comprehensive structural model for Nd- and Ga-doped sulfide glasses is proposed.

DOI: 10.1103/PhysRevB.81.104204

PACS number(s): 61.43.Bn, 42.70.Hj, 32.50.+d

## I. INTRODUCTION

Rare earth (RE)-doped chalcogenide glasses are of great interest for applications such as fiber-optic amplifiers<sup>1</sup> for telecom networks, and planar-waveguide amplifiers<sup>2</sup> for integrated optical circuits. In such devices, it is of crucial importance to improve the RE solubility in glasses to achieve high gain characteristics. This is especially true for planar-waveguide-type optical amplifiers because of the short interaction length of the gain medium.<sup>3</sup> Chalcogenide glasses, however, exhibit low RE solubilities,  $\sim 10^2$  ppm (Ref. 4); therefore strong concentration quenching prevails even at low RE concentrations.

It is known that poor RE solubility, and subsequent strong concentration quenching, can be substantially improved by incorporating Ga into chalcogenide glasses.<sup>5</sup> However, in spite of its importance, few studies<sup>6,7</sup> of the microscopic mechanism of the Ga-doping effect have yet been made, and the actual atomistic changes involved are still unknown. This is presumably due to difficulties associated with the low RE concentrations involved, as well as the intrinsic disordered nature of amorphous solids. New approaches are therefore required to understand the role of Ga on the microscopic scale. This is essential for further improvement in the performance of optical amplifiers or lasers and also for deepening our understanding of the microscopic behavior of RE-doped chalcogenide glasses.

In this paper, we report strong evidence for a spatial correlation between RE ions and GaS<sub>4</sub> tetrahedra in chalcogenide glasses by using laser spectroscopy and *ab initio* molecular dynamics (AIMD) simulations. It is argued here that such a correlation results from the formation of Ga-rich phases in which RE ions reside homogeneously without clustering. This microscopic structural model provides insights into the crucial question of how Ga can improve the solubility and fluorescence properties of RE ions in chalcogenide glasses.

## II. EXPERIMENTAL AND COMPUTATIONAL METHODS

The base “GAGS” glass compositions investigated in this study were Ge<sub>23.5</sub>As<sub>(11.8-x)</sub>Ga<sub>x</sub>S<sub>64.7</sub> ( $0 \leq x \leq 3$ ) [i.e., (GeS<sub>2</sub>)<sub>4</sub>(As<sub>2</sub>S<sub>3</sub>) for  $x=0$ ]. Glass samples were fabricated by a conventional melt-quenching method for chalcogenide glasses.<sup>8</sup> The time evolution of fluorescence and excitation spectra were obtained using a Ti-sapphire laser combined with a monochromator, an InGaAs detector, and an oscilloscope or a lock-in amplifier. Further details of sample fabrication and optical measurements are described elsewhere.<sup>8</sup> The maximum Nd<sup>3+</sup> doping concentration without devitrification was found to be  $\sim 0.02$  at. % in Ga-free glass ( $x=0$ ) and increases with Ga doping; e.g., it is 0.06 and 0.12 at. % for  $x=0.6$  and 1.2 at. %, respectively. Such devitrification is due to either phase separation or crystallization and, thus, it can be seen that Ga atoms tend to stabilize the glass structure against phase transitions induced by RE doping.

MD simulations were carried out using both the Vienna *Ab initio* Simulation Package (VASP), in which theoretical calculations are based on density functional theory (DFT),<sup>9</sup> and the density functional-based tight binding (DFTB) (Ref. 10) method. Models of 100 atoms were simulated using VASP at constant volume in cubic supercells with periodic boundary conditions. The total energy of the models was calculated at the gamma point with Gaussian smearing. The projector augmented-wave method, with the Perdew-Burke-Ernzerhof exchange-correlation functional, was employed.<sup>11,12</sup> The plane-wave energy cutoff was set at 194 eV. The outer *s* and *p* electrons were treated as valence electrons, while Nd atoms were assumed to be in the trivalent ionic state and their 4*f* states were treated as core states. MD simulations for a model of 200 atoms were performed using the DFTB method, which is derived from full DFT by a second-order expansion of the energy functional around a suitable reference density.<sup>13</sup> Although DFTB uses more approximations

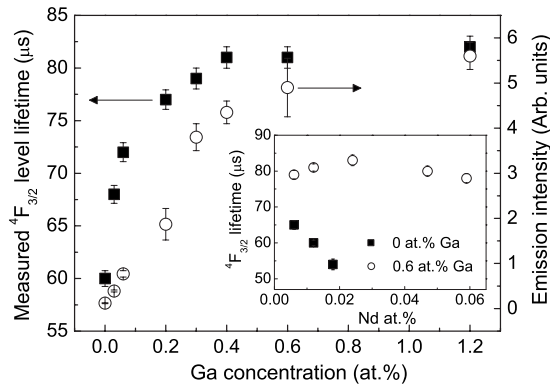


FIG. 1. Changes with Ga concentration in the room-temperature  $\text{Nd}^{3+}$ :  ${}^4\text{F}_{3/2}$  level lifetimes and fluorescence intensities in Nd-doped GAGS glasses, measured at 1080 nm. The  $\text{Nd}^{3+}$  concentration was 0.01 at. %. The inset shows the lifetime of the same level for different  $\text{Nd}^{3+}$  concentrations.

than DFT, the accuracy of DFTB is close to full DFT calculations, as has been shown in various benchmark studies.<sup>14,15</sup> Further details of simulation methods for DFTB can be found elsewhere.<sup>10,16</sup> The integration time step was 3 or 5 fs for VASP and 5 fs for DFTB. The experimental density at room temperature (2.92 g/cm<sup>3</sup>) was used in the simulations. These AIMD simulations have been previously used successfully by us to investigate, e.g., defects<sup>17</sup> and atomic structures and crystallization<sup>18</sup> in chalcogenide glasses.

### III. SPECTROSCOPIC EVIDENCE OF SPATIAL CORRELATION

#### A. Fluorescence lifetime and intensity variation

Optical absorption spectra were measured for glasses with different Ga concentrations. From the measured absorption cross sections, oscillator strengths for all the ground-state transitions of  $\text{Nd}^{3+}$  ions were evaluated. The calculated oscillator strengths were found to be essentially identical within experimental error, implying that the radiative transition probabilities ( $A_R$ ) of  $\text{Nd}^{3+}$  levels are insensitive to Ga doping, at least up to 3 at. % of Ga. The  ${}^4\text{F}_{3/2}$ -level lifetimes and fluorescence intensities measured for 1080 nm emission were also monitored at several different Ga concentrations while the  $\text{Nd}^{3+}$  concentration ( $n_{\text{Nd}}$ ) was kept fixed at 0.01 at. % for comparison (Fig. 1). The lifetime shows an initial sharp increase and then saturates for Ga concentration greater than 0.4 at. %. A similar trend is also observed for the fluorescence intensity change, as shown in Fig. 1. The origin of these radical increases in lifetimes and fluorescence intensities can be attributed to the decrease in  $\text{Nd}^{3+}$ - $\text{Nd}^{3+}$  energy-transfer rates ( $A_{ET}$ ), since other important factors affecting measured lifetimes (e.g., radiative transition and multiphonon relaxation rates) are not sensitive to such small amounts of Ga doping. The onset of energy transfer for the Ga-free sample is confirmed from the observed concentration quenching of the  ${}^4\text{F}_{3/2}$ -level lifetime, as shown in the inset of Fig. 1. The main energy-transfer processes responsible for this concentration quenching can be cross relaxation medi-

ated by an excitation-migration process.<sup>19</sup> Providing Dexter-type resonant<sup>20</sup> and/or nonresonant<sup>21</sup> processes of an electric dipole-dipole nature are dominant, the energy-transfer rate should be proportional to  $R^{-6}$ , where  $R$  is the separation between donor and acceptor  $\text{Nd}^{3+}$  ions. Hence the essential role of Ga, deduced from the present results, is to increase the average atomic distances between nearby  $\text{Nd}^{3+}$  ions, resulting in a subsequent decrease in  $A_{ET}$ .

The significance of the results in Fig. 1 is that there is a striking discrepancy between the magnitude of the lifetime and fluorescence-intensity variations. Since the measured fluorescence intensities are proportional to measured lifetimes of fluorescent levels under our experimental conditions (constant  $A_R$  and  $n_{\text{Nd}}$ ), the fluorescence intensity increase up to 0.6 at. % of Ga doping is thus expected to be only  $\sim 30\%$  of that of the Ga-free glass, which is much smaller than that actually observed ( $\sim 60$  times). A convincing structural model able to explain this result involves the formation of tightly bound RE clusters (in the Ga-free glass), in which RE ions are so close that most excited ions are relaxed to lower states via energy-transfer processes.<sup>22</sup> Another striking observation is that the lowest concentration of Ga (0.03 at. %) is able to cause an appreciable increase in lifetime ( $\sim 10\%$ ) and fluorescence intensity (approximately three times) from as low a concentration of Nd as 0.01 at. %. This result strongly suggests that incorporated Ga atoms are spatially correlated with  $\text{Nd}^{3+}$  ions in clusters.<sup>6,7</sup> The hypothesis of such a correlation can be tested by tracking the variations in local structures around  $\text{Nd}^{3+}$  ions with small amounts of Ga doping.

#### B. Site-selective spectroscopy

We have therefore monitored changes in site-selective excitation spectra in order to probe local structural changes around  $\text{Nd}^{3+}$  ions. To avoid any complexity arising from thermal excitation of upper Stark sublevels of manifolds, the sample temperature was kept at 12 K. Figure 2(a) shows excitation spectra for  $x=0$  and 0.2 at. % Ga-doped glasses measured at different emission wavelengths.

In the case of the Ga-free glass, all the excitation spectra measured over the  ${}^4\text{F}_{3/2} \rightarrow {}^4\text{I}_{11/2}$  emission band are well resolved into two Gaussian peaks, which might correspond to transitions from the lowest Stark sublevel of the  ${}^4\text{I}_{9/2}$  manifold to two sublevels of the  ${}^4\text{F}_{3/2}$  manifold (the maximum number of Stark sublevels for this manifold). From crystal-field theory,<sup>23</sup> the appearance of a maximum number of peaks could be interpreted as indicating the presence of a primary  $\text{Nd}^{3+}$  site with a site symmetry lower than cubic. Such primary sites have also been identified in other glass systems.<sup>24</sup> In contrast, the 0.2 at. % Ga-doped glass shows two pronounced changes in the excitation spectra. First, the spacing between peaks, i.e., the magnitude of the Stark splittings, becomes smaller, presumably due to a decrease in the ligand-field strength experienced by  $\text{Nd}^{3+}$  ions. Second, as the emission wavelength moves to the higher energy side of the emission band, more than two peaks are clearly observed; the spectra are well fitted by four Gaussian peaks rather than two.

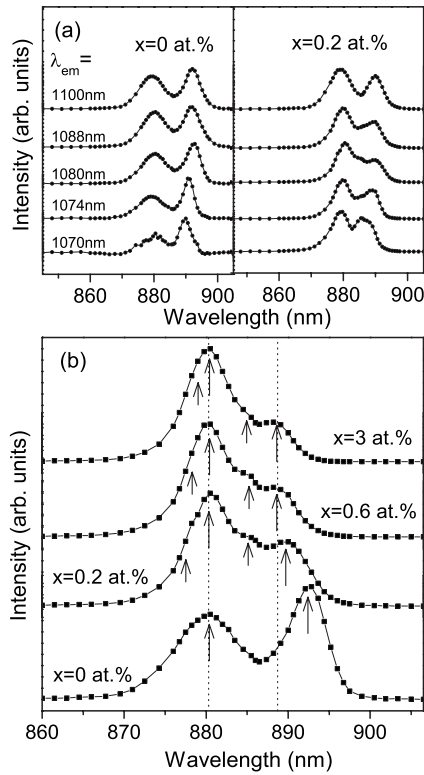


FIG. 2. (a) Excitation spectra of the  ${}^4F_{3/2} \rightarrow {}^4I_{11/2}$  emission transitions for two different Ga-dopant concentrations ( $x$ ) in GAGS glasses. The  $\text{Nd}^{3+}$  concentration was fixed at 0.01 at. %. Each spectrum was measured at 12 K and at the different emission wavelengths specified. (b) Excitation spectra for Ga-doped glasses measured at 1080 nm. The arrows indicate the center positions of fitted Gaussian peaks.

This trend is more clearly revealed by comparing the excitation spectra measured at the peak emission wavelength, 1080 nm, as shown in Fig. 2(b). The implication of this result is as follows. As expected, there is a large change in ligand structure around  $\text{Nd}^{3+}$  ions upon Ga doping. This modification of  $\text{Nd}^{3+}$  sites is such that two distinguishable sites (inferred from the four peaks) are likely to be formed with ligand structures different from those in Ga-free glass, as evidenced from the different peak positions and intensity ratios. Most modification then ends when the Ga concentration exceeds  $\sim 0.6$  at. %, as revealed from the close similarity in excitation spectra between the 0.6 and 3 at. % Ga-doped glasses. Although not measured at 1080 nm, the spectrum of the 0.03 at. % Ga-doped glass also shows four such peaks at emission wavelengths shorter than 1070 nm (not shown), in contrast to the two peaks observed in the Ga-free glass. Therefore, it seems reasonable to assume that the variation in excitation spectra, along with lifetime and emission-intensity changes, at such low Ga-doping levels is a strong indication of spatial correlations between Ga and  $\text{Nd}^{3+}$  ions, leading to  $\text{Nd}^{3+}$  local structural changes as well as a redistribution of  $\text{Nd}^{3+}$  ions. This then raises the question of the possible origin of such correlations. In addition, more specific information on the Ga and Nd atomic configurations is required to present a comprehensive atomic structural model for Ga-Nd co-doped glasses.

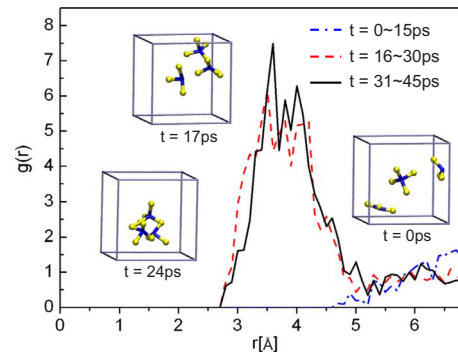


FIG. 3. (Color online) Partial RDF curves for the Ga-Ga pair in the  $\text{Ga}_3\text{Nd}$  liquid at 1300 K. RDF curves obtained from atomic configurations were averaged over the time intervals indicated in the figure. Atomic configurations at three different simulation times are also shown as an example. Blue or yellow balls and sticks represent Ga or S atoms and their bonding. Other atoms are not shown for clarity.

#### IV. *AB INITIO* MOLECULAR-DYNAMICS SIMULATION STUDY

##### A. Spatial correlation between $\text{GaS}_4$ units

In order to gain an insight into these questions, we have first carried out AIMD simulations on a number of glass compositions using the VASP code, mainly  $\text{Ge}_{23}\text{As}_8\text{Ga}_3\text{S}_{65}\text{Nd}_1$  ( $\text{Ga}_3\text{Nd}$ ) and  $\text{Ge}_{23}\text{As}_5\text{Ga}_6\text{S}_{65}\text{Nd}_1$  ( $\text{Ga}_6\text{Nd}$ ). The average coordination number (CN) of the amorphous 100-atom models produced by AIMD simulation is 3.9 for Ge and 3.1 for As atoms, consistent with the 8-N rule.<sup>25</sup> More significantly, this simulation reproduced the fourfold coordination (CN=4.0) of Ga atoms, in agreement with EXAFS.<sup>26</sup> This abnormal CN of Ga, i.e., the formation of  $\text{GaS}_4$  tetrahedra, has often been invoked to explain the high RE solubility of Ga-doped glasses.<sup>6,7</sup>

A key finding from these MD simulations is that a strong tendency for clustering of  $\text{GaS}_4$  tetrahedra was found for both  $\text{Ga}_3\text{Nd}$  and  $\text{Ga}_6\text{Nd}$  simulations in the liquid state. Figure 3 shows snapshots taken at several simulation times for the  $\text{Ga}_3\text{Nd}$  glass as well as radial-distribution function (RDF) curves for Ga-Ga atom pairs. It can be seen from the snapshots that Ga atoms in the initial configuration ( $t=0$ ) are almost homogeneously distributed in the liquid and then later form a pair of Ga tetrahedra ( $t=17$  ps), followed by the formation of a cluster ( $t=24$  ps). The evolution of the RDF curves, averaged over the time intervals given in the figure, more clearly reveals such a tendency for Ga clustering. The coordination number for the presumably second-nearest neighbor of Ga atoms, calculated from the first Ga-Ga correlation peak, turns out to be 1.1, indicating that, during most of the simulation time after 15 ps,  $\text{GaS}_4$  units tend to remain close together to form pairs, chains or rings by corner or edge sharing. This simulation result suggests that the formation of such clusters is energetically more favorable than stochastic mixing in the liquid, which might be understood in a broad sense as indicating phase separation of Ga-rich regions in the liquid.

AIMD simulations using the DFTB method (at 2000 K) have also been performed for a model with a composition of

$\text{Ge}_{47}\text{As}_{17}\text{Ga}_6\text{S}_{130}$  (Ga6). In this case, to get statistically more significant results, we simulated a 200-atom model for a much longer simulation time ( $\sim 450$  ps) than those using VASP. The general trend obtained from the DFTB simulations was basically very similar to the VASP simulation results of a 100-atom model, that is, clusters of Ga tetrahedra were persistently formed and, in many cases, lasted for several tens of picoseconds in the liquid. The close similarity of results obtained from these two different simulational approaches, with different system sizes, reinforces our hypothesis of the formation of Ga-rich regions proposed principally from DFT-based MD simulations.

### B. Spatial correlation between Nd and $\text{GaS}_4$ units

The analysis using partial radial-distribution functions  $g(r)$  for revealing correlations between  $\text{GaS}_4$  units in the preceding section was not able to provide statistically meaningful outcomes in this case because of the small number of Nd atoms in the model. Instead, in order to probe the spatial correlation between Nd and Ga atoms, we analyzed the time-dependent positions of atoms in the liquid using the distinct part of the van Hove correlation function [ $G_d(r,t)$ ], which is generally defined as

$$G_d^{\alpha\beta}(r,t) = \frac{1}{\sqrt{N_\alpha N_\beta}} \sum_{i=1}^{N_\alpha} \sum_{j=1}^{N_\beta} \langle \delta[\mathbf{r} - \mathbf{r}_i^\alpha(0) + \mathbf{r}_j^\beta(t)] \rangle. \quad (1)$$

Here,  $\mathbf{r}_i^\alpha(t)$  and  $\mathbf{r}_j^\beta(t)$ , respectively, denote the position of particle  $i$  of species  $\alpha$  and particle  $j$  of species  $\beta$  at time  $t$ .  $N_\alpha$  and  $N_\beta$  are the number of particles of species  $\alpha$  and  $\beta$ , respectively. At  $t=0$ ,  $G_d^{\alpha\beta}(r,t)$  is proportional to the partial radial-distribution function  $g_{\alpha\beta}(r)$ . This function can provide information on the relative movement between different types of atoms, especially the gradual breakup of the initial structure, during MD simulations.<sup>27</sup> If there is any interaction between two different species of atoms (or two different structural units), this function may give some indication of the spatial correlations in terms of a different decay behavior of an initial partial radial-distribution function as a function of time.

A central observation from this analysis was that, regardless of the choice of initial configuration during the simulation, Nd-Ga pairs in the Ga6Nd liquid show a considerably slower decay of the first Nd-Ga correlation peak (at  $\sim 4$  Å) in  $G_d(r,t)$  compared to any other (non-Ga-S) combination of atomic pairs. As an example, Fig. 4 shows the evolution of  $G_d(r,t)$  at successive time intervals for Nd-As and Nd-Ga pairs. Such a memory effect in diffusion, even in a highly mobile liquid, naturally suggests a correlation in the trajectory of Ga and  $\text{Nd}^{3+}$  ions as a result of an interaction between them (or their polyhedra), which, when quenched into the glass, is, in turn, presumably related to the spatial correlation as observed from spectroscopic measurement.

From our lifetime data shown in Fig. 1, the observed lowest Ga/Nd ratio for the Ga-Nd correlation to be manifested was  $\sim 3$ . Taking account of the initial sharp increase in lifetime with Ga doping, the actual Ga-Nd correlation appears to start for a ratio even much smaller than this. In our MD

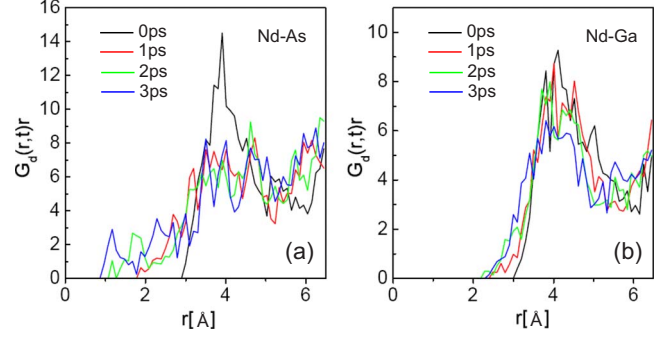


FIG. 4. (Color online) Distinct part of the van Hove correlation functions for (a) Nd-As and (b) Nd-Ga pairs. These figures were obtained at four successive time intervals during AIMD simulations for the Ga6Nd liquid at 1300 K.

simulations, such a correlation was observed only for the Ga6Nd model, as shown in Fig. 4, while no clear evidence of a correlation was found in the case of the Ga3Nd model for which the Ga/Nd ratio is 3. Although this result might indicate a certain degree of dependence of the Ga-Nd correlation on the Ga/Nd concentration ratio, as observed in experiment,<sup>7</sup> our simulation method is not appropriate to extract quantitatively meaningful information comparable to experiments on this behavior due to the limited system size and time scale employed. Nevertheless, the unique departure from ordinary decay times observed for the Ga-Nd pair clearly implies the presence of a microscopic interaction between Ga and Nd atoms (or their polyhedra), presumably resulting in the spatial correlation as observed in experiments.

It is interesting to consider the size of systems in MD simulations necessary directly to observe significant Nd-Ga correlations, e.g., in partial radial-distribution functions. The approximate minimum system size can be inferred from the average Nd-Nd interatomic distances estimated by a microscopic (hopping) model for energy transfer.<sup>8,28</sup> Providing only 1% of total  $\text{Nd}^{3+}$  ions are relaxed nonradiatively by energy transfer (representing Nd and Ga co-doped glasses), and using a typical critical distance (7 Å) for cross relaxation and excitation migration,<sup>19</sup> the  $\text{Nd}^{3+}$  concentration under this condition is approximately  $\sim 8 \times 10^{19} \text{ cm}^{-3}$  which, in turn, corresponds to an average interatomic distance of  $\sim 23$  Å. This is clearly too large for the Nd-Ga correlations directly observed in the small models currently simulated by our *ab initio* MD.

## V. DISCUSSION

The evolution of radial-distribution functions and van Hove correlation functions (Fig. 4) suggest that the nature of spatial correlations might be closely related to the interaction between near-neighbor atoms, i.e., Ga and Ga (or Nd and Ga), or more likely their polyhedra, during diffusion in the liquid. Therefore, it would be interesting to investigate the dynamical aspects of the bond formation and annihilation during MD simulations, considering up to second-nearest-neighbor atoms. As a way of doing this, we have calculated

TABLE I. Average bond-duration times (given in fs) for several different types of bonds formed in liquid during MD simulations. The center atom (S) is bridging the other two atoms, and the bond-duration time was determined when any one of (or both) bonds with these two atoms are broken. It was then averaged for all this type of bonds formed during MD simulations.

Model	Method	Types of bonds							
		Ge-S-Ge	As-S-As	Ga-S-Ga	Ga-S-Ge	Ga-S-As	Nd-S-Ge	Nd-S-As	Nd-S-Ga
Ga3Nd	DFT	198	165	561	297	252	314	342	409
Ga6Nd	DFT	206	216	569	305	257	325	388	518
Ga6	DFTB	178	156	335	247	260			

a bond-duration time ( $\tau_b$ ) for each type of bond, and averaged this for all of the same types of bonds formed in MD simulations.<sup>29</sup> The average values of  $\tau_b$ s so calculated are presented in Table I for several different types of bonds.

We can first notice from the first five types of bonds (including no Nd atom) in Table I that there is a significant difference in  $\tau_b$  between Ga-S-Ga and other types of bonds, e.g., Ge-S-Ge and As-S-As. In the case of models generated by the DFT method,  $\tau_b$  for the former is about two or three times longer than those for the latter whereas a less significant, but still meaningful, difference was found in DFTB-based MD simulations. This result clearly indicates that, once chemical bonds between GaS<sub>4</sub> tetrahedral units form in the liquid, they, on average, last much longer than bonds between other structural units, such as GeS<sub>4</sub> or AsS<sub>3</sub>. The main parameters determining  $\tau_b$  may be the thermal energy  $k_B T$  and the bond strength between S and other atoms. Hence, stronger bonds between Ga and S compared to other bonds are expected from these results. Such a difference in the bond strength is then likely to lead to the formation of clusters of GaS<sub>4</sub> tetrahedra in that less frequent bond breakages of Ga-S-Ga should increase the probability of aggregation of GaS<sub>4</sub> units in the liquid, as observed in our MD simulations. In larger systems, the concentration of Ga atoms, as well as their diffusion coefficient, would be other important factors affecting the degree of clustering in the liquid; thus a kinetic factor would play an important role in this case.

A similar explanation might be given to explain the correlation between Ga and Nd atoms, since  $\tau_b$  for Nd-S-Ga is larger than for other Nd-related bonds, as shown in Table I. Interestingly, this trend is clearly identified for the Ga6Nd model, and less significant for Ga3Nd, which is consistent with the results from the evolution of the van Hove correlation functions. Besides this kinetics-based model, thermodynamic models, e.g., phase separation, might be considered to explain the experimentally observed spatial correlations, although our MD simulations are not able to distinguish the degree of relevance of each model.

Nevertheless, our *ab initio* MD simulations, as well as spectroscopic measurements, have revealed an apparent spatial correlation between Ga and Nd atoms. In addition, GaS<sub>4</sub> clusters were found to be favorable structural elements constituting the liquid mixture. These two observations make it possible for us to suggest a reasonable structural model of how Ga atoms, even a very small portion of them, are able to facilitate the high solubility of RE ions and enhance their

fluorescence properties. In the case of the Ga-free glass, most Nd<sup>3+</sup> ions are likely to be in their clusters.<sup>22</sup> Provided that 99% of Nd<sup>3+</sup> ions relax nonradiatively by energy transfer,  $n_{Nd}$  is approximately  $\sim 2.8 \times 10^{21} \text{ cm}^{-3}$ , which corresponds to an average interatomic distance of  $\sim 5 \text{ \AA}$ . This estimated distance, close to the observed minimum RE-RE distance found in oxide glasses,<sup>30</sup> corresponds approximately to the Nd-S-Nd configuration. As the Ga concentration increases, however, these clusters are resolved into Ga-rich regions rather than Ge-As-rich regions and then become fully dispersed once the proportion of such Ga-rich regions reaches a certain critical value. This structural model, i.e., the formation of a Ga-rich phase and the preferential dissolution of RE ions in this region, can be rationalized by the fact that gallium and lanthanum sulfides form stable glasses, known as GLS, which show a considerably higher RE solubility than other Ge- or As-based chalcogenide glasses.<sup>31</sup>

We have performed EXAFS experiments at all the *K* edges of the elements in RE-doped GAGS glasses and at the *L*<sub>III</sub> edges for RE ions. Although we see changes in the local structure (e.g., an increase in RE-S distance with Ga-doping), this technique is not sensitive to *next*-nearest-neighbor correlations in glasses, which could otherwise provide experimental structural evidence for Nd-Nd or Nd-Ga cluster correlations.

## VI. CONCLUSIONS

In summary, a preferential spatial correlation between Nd<sup>3+</sup> and GaS<sub>4</sub> units has been proposed to explain significant changes in spectroscopic properties, as well as in the ligand structure of Nd<sup>3+</sup> ions, for low Ga doping in chalcogenide glasses. Such a correlation, along with a strong tendency for formation of Ga-tetrahedra clusters, provides a comprehensive atomistic structural model for rare earth and Ga codoped chalcogenide glasses.

## ACKNOWLEDGMENTS

T. H. Lee is grateful for a Korea Research Foundation Grant (MOEHRD) (Grant No. KRF-2006-352-D00102), J. Hegedus for support from the European Union (Marie Curie Actions), and J. Heo for Grant No. KRF-2005-005-J13101. Financial support by the UK Home Office is gratefully acknowledged. VASP simulations were performed using the Cambridge High-Performance Computer Facility.

- <sup>1</sup>Rare Earth Doped Fiber Lasers and Amplifiers, edited by M. J. F. Digonet (Dekker, New York, 1993).
- <sup>2</sup>See, e.g. J. A. Frantz, L. B. Shaw, J. S. Sanghera, and I. D. Aggarwal, *Opt. Express* **14**, 1797 (2006).
- <sup>3</sup>P. G. Kik and A. Polman, *MRS Bull.* **23**, 48 (1998).
- <sup>4</sup>D. R. Simons, A. J. Faber, and H. de Waal, *J. Non-Cryst. Solids* **185**, 283 (1995).
- <sup>5</sup>See, for example, K. Wei, D. P. Machewirth, J. Wenzel, E. Snitzer, and G. H. Sigel, Jr., *Opt. Lett.* **19**, 904 (1994).
- <sup>6</sup>J. Heo, J. M. Yoon, and S. Y. Ryou, *J. Non-Cryst. Solids* **238**, 115 (1998).
- <sup>7</sup>B. G. Aitken, C. W. Ponader, and R. S. Quimby, *C. R. Chim.* **5**, 865 (2002).
- <sup>8</sup>T. H. Lee and J. Heo, *Phys. Rev. B* **73**, 144201 (2006).
- <sup>9</sup>G. Kresse and J. Hafner, *Phys. Rev. B* **47**, 558 (1993).
- <sup>10</sup>T. Frauenheim, G. Seifert, M. Elstner, T. Niehaus, C. Köhler, M. Amkreutz, M. Sternberg, Z. Hajnal, A. D. Carlo, and S. Suhai, *J. Phys.: Condens. Matter* **14**, 3015 (2002).
- <sup>11</sup>G. Kresse and D. Joubert, *Phys. Rev. B* **59**, 1758 (1999).
- <sup>12</sup>J. P. Perdew, K. Burke, and M. Ernzerhof, *Phys. Rev. Lett.* **77**, 3865 (1996).
- <sup>13</sup>M. Elstner, D. Porezag, G. Jungnickel, J. Elsner, M. Haugk, T. Frauenheim, S. Suhai, and G. Seifert, *Phys. Rev. B* **58**, 7260 (1998).
- <sup>14</sup>N. Otte, M. Scholten, and W. Thiel, *J. Phys. Chem. A* **111**, 5751 (2007).
- <sup>15</sup>H. Witek and K. Morokuma, *J. Comput. Chem.* **25**, 1858 (2004).
- <sup>16</sup>S. I. Simdyankin, S. R. Elliott, Z. Hajnal, T. A. Niehaus, and T. Frauenheim, *Phys. Rev. B* **69**, 144202 (2004).
- <sup>17</sup>S. I. Simdyankin, T. A. Niehaus, G. Natarajan, T. Frauenheim, and S. R. Elliott, *Phys. Rev. Lett.* **94**, 086401 (2005).
- <sup>18</sup>J. Hegedus and S. R. Elliott, *Nature Mater.* **7**, 399 (2008).
- <sup>19</sup>See, for example, A. S. S. de Camargo, E. R. Botero, D. Garcia, J. A. Eiras, and L. A. O. Nunes, *Appl. Phys. Lett.* **86**, 152905 (2005) and references therein.
- <sup>20</sup>D. L. Dexter, *J. Chem. Phys.* **21**, 836 (1953).
- <sup>21</sup>T. Miyakawa and D. L. Dexter, *Phys. Rev. B* **1**, 2961 (1970).
- <sup>22</sup>T. H. Lee, S. I. Simdyankin, L. Su, and S. R. Elliott, *Phys. Rev. B* **79**, 180202(R) (2009).
- <sup>23</sup>C. Gorller-Walrand and K. Binnemans, in *Handbook on the Physics and Chemistry of Rare Earths*, edited by K. A. Gschneidner, Jr. and L. Eyring (Elsevier, Amsterdam, 1998), Vol. 25 (and references therein).
- <sup>24</sup>C. C. Robinson and J. T. Fournier, *J. Phys. Chem. Solids* **31**, 895 (1970).
- <sup>25</sup>N. F. Mott and E. A. Davis, *Electronic Processes in Non-crystalline Materials* (Clarendon Press, Oxford, 1979).
- <sup>26</sup>A. M. Loireau-Lozac'h, F. Keller-Besrest, and S. Benazeth, *J. Solid State Chem.* **123**, 60 (1996).
- <sup>27</sup>W. K. Kegel and A. van Blaaderen, *Science* **287**, 290 (2000).
- <sup>28</sup>D. F. de Sousa and L. A. O. Nunes, *Phys. Rev. B* **66**, 024207 (2002) and references therein.
- <sup>29</sup>For this calculation, we defined a bond between two atoms once their separation was shorter than a radial distance cutoff ( $R_{cut}$ ) that was appropriately determined from the partial radial-distribution function for corresponding atom pairs. For example,  $R_{cut}$  values used in the calculations were 2.85 Å for Ga-S and As-S, 2.95 Å for Ge-S, and 3.50 Å for Nd-S pair atoms. It turned out that, although  $\tau_b$  depended more or less on the value of  $R_{cut}$  used, the main conclusion from this analysis was not affected by a variation of  $R_{cut}$  within a reasonable range.
- <sup>30</sup>J. M. Cole, A. C. Hannon, R. A. Martin, and R. J. Newport, *Phys. Rev. B* **73**, 104210 (2006).
- <sup>31</sup>R. Reisfeld and A. Bornstein, *J. Non-Cryst. Solids* **27**, 143 (1978).